Am J Cancer Res 2021;11(12):6004-6023
www.ajcr.us /ISSN:2156-6976/ajcr0129479

Original Article

Legacy effect of high glucose on promoting survival of HCT116 colorectal cancer cells by reducing endoplasmic reticulum stress response

Heung Man Lee[1,2], Shao Chin Lee[1,2,5], Lan He[1,2], Alice Pik Shan Kong[1,2,3], Dandan Mao[1,2], Yong Hou[1,2], Arthur Chi Kong Chung[4], Gang Xu[1,2,3], Ronald Ching Wan Ma[1,2,3], Juliana Chung Ngor Chan[1,2,3]

[1]Department of Medicine and Therapeutics, [2]Li Ka Shing Institute of Health Sciences, [3]Hong Kong Institute of Diabetes and Obesity, The Chinese University of Hong Kong, Prince of Wales Hospital, Shatin, Hong Kong; [4]Department of Chemistry, Hong Kong Baptist University, Hong Kong; [5]Department of Biological Sciences, School of Life Sciences, Shanxi University, Taiyuan 030006, Shanxi, China

Received January 3, 2021; Accepted October 25, 2021; Epub December 15, 2021; Published December 30, 2021

Abstract: Patients with diabetes have increased risk of cancer and poor response to anti-cancer treatment. Increased protein synthesis is associated with endoplasmic reticulum (ER) stress which can trigger the unfolded protein response (UPR) to restore homeostasis, failure of which can lead to dysregulated cellular growth. We hypothesize that hyperglycemia may have legacy effect in promoting survival of cancer cells through dysregulation of UPR. Using HCT116 colorectal cancer cells as a model, we demonstrated the effects of high glucose (25 mM) on promoting cell growth which persisted despite return to normal glucose medium (5.6 mM). Using the Affymetrix gene expression microarray in HCT116 cells programmed by high glucose, we observed activation of genes related to cell proliferation and cell cycle progression and suppression of genes implicated in UPR including BiP and CHOP. These gene expression changes were validated in HCT116 cancer cells using quantitative real-time PCR and Western blot analysis. We further examined the effects of thapsigargin, an anti-cancer prodrug, which utilized ER stress pathway to induce apoptosis. High glucose attenuated thapsigargin-induced UPR and growth inhibition in HCT116 cells, which persisted despite return to normal glucose medium. Western blot analysis showed activation of caspase-3 in thapsigargin-treated cells in both normal and high glucose medium, albeit with lower levels of cleaved caspase-3 in cells exposed to high glucose, suggesting reduced apoptosis. Flow cytometry analysis confirmed fewer apoptotic cells under thapsigargin treatment in cells exposed to high glucose. Our results suggested that hyperglycemia altered gene expression involved in UPR with increased cell proliferation and facilitated survival of HCT116 cells under thapsigargin-induced ER stress by reducing the apoptotic response.

Keywords: Apoptosis, cancer, diabetes, ER stress, UPR

Introduction

The increased risk of cancer death in type 2 diabetes (T2D) has been reported as early as 1914 [1] supported by large scale cohort analysis [2-4]. In the Hong Kong Diabetes Register (HKDR), which was a research-driven quality improvement program established since 1995 with documentation of risk factors, complications and clinical outcomes [5], one in four patients with T2D died with cancer. This was in part driven by aging and increasing survival from cardiovascular-renal complications [6]. About half of these cancer-associated deaths came from the gastrointestinal system with liver cancer and colorectal cancer being the most dominant causes [7].

T2D is characterized by chronic hyperglycemia with varying contributions from insulin resistance and insulin deficiency. In a matched prospective cohort analysis of patients with T2D, we were among the first to report the linear associations between all-cancer risk and glycated haemoglobin (HbA1c) [8]. In a global analysis of published data up to 2017, it was estimated that 5.6% of all incident cancers in 2012 were attributable to the combined eff-

ects of diabetes and obesity, corresponding to 792,600 new cases [9].

Cancer cells are mutated cells with abnormal growth potential and characteristics. Cancer cells prefer to use glucose as the energy source for growth [10-12]. In experimental studies, cancer cells exhibited high growth potentials in high glucose medium with increased expression of genes that promoted cell cycle progression and cell proliferation [13, 14]. High glucose treatment also induced stress in cells with specialized function such as pancreatic β cells and cytokine-producing cells [15-17]. In these specialized cells, high glucose induced endoplasmic reticulum (ER) stress with increased expression of genes such as BiP and CHOP.

ER is the organelle for protein maturation through adopting a three-dimensional structure with post-translational modification including glycosylation and proteolytic cleavage. Under ER stress, these processes are disrupted and the ER is filled with unfolded proteins, which may activate the unfolded protein response (UPR) that can culminate to cellular apoptosis. BiP is the chaperone protein located in the ER [18], which under ER stress, binds to the unfolded proteins and releases its binding partners, PERK and IRE1. Upon phosphorylation, the released PERK and IRE1 activate transcription factors such as ATF4 and XBP1 to increase the expression of BiP and CHOP [19, 20]. While CHOP is the key transcription factor that regulates gene expression to facilitate the cells to survive, it can also activate genes that lead to apoptosis should the initial response to ER stress fail [21].

Both cancer and diabetes are associated with dysregulation of protein metabolism. In cancer cells, adaptive UPR during ER stress may promote cellular growth [22] while in diabetes and obesity, increased UPR during ER stress may cause cellular death in fully differentiated cells [23]. Under metabolic stress, UPR is activated due to accumulation of unfolded or misfolded proteins in the ER. The UPR aims to restore normal cellular function by halting protein translation, degrading misfolded proteins, increasing the production of molecular chaperones involved in protein folding, or inducing apoptosis if these processes are overwhelmed [22].

Despite the high risk of cancer in diabetes, there have been few studies examining the roles of ER stress on cancer growth in high glucose condition. Given the burden of colorectal cancer in T2D, we used HCT116 colorectal cancer cells as a cell culture model [24] and hypothesized that ER stress might underlie the dysregulation of cell growth and apoptosis in high glucose condition. Using the Affymetrix gene expression microarray, we observed high glucose suppressed genes implicated in ER function, including BiP and CHOP, whilst activated genes related to cell proliferation and cell cycle progression. We further examined the effects of the calcium influx blocker, thapsigargin, which had anti-cancer potential by inducing ER stress and apoptosis, on HCT116 cells. High glucose attenuated the growth inhibition and ER stress induced by thapsigargin on HCT116 cells with reduced apoptosis, which persisted despite return to normal glucose medium.

Materials and methods

Cell culture conditions and drug treatment

Human HCT116 colorectal cancer cells [24] were kindly provided by Professor Anthony Lo (Department of Anatomical and Cellular Pathology, The Chinese University of Hong Kong). The HCT116 cancer cells were cultured in DMEM medium containing normal glucose (5.6 mM) or high glucose (25 mM), 10% fetal bovine serum (FBS), 50 μg/ml penicillin-streptomycin in CO_2 incubator at 37°C. During the experiments, the cells were plated out in the normal glucose medium and allowed to settle for 1 day. After 1 day, the cells were fasted in normal glucose medium containing antibiotics but without FBS (serum free medium, SFM) for 24 hours. After fasting, the cells were treated either in normal glucose medium or DMEM medium with 25 mM glucose or desired glucose concentration containing 10% FBS (high glucose medium) and antibiotics. As control, the cells were treated with normal glucose medium as well as normal glucose plus mannitol to control for the effects of osmolality due to high glucose. Cells were treated for 24 hours or desired time period and then harvested for experiment. For treatment with drugs, thapsigargin was purchased from Sigma (St. Louis, MO, USA). HCT116 cells were plated out and allowed to settle for 1 day in normal glucose medium. The cells were then fasted in SFM for 24 hours before changing to either normal glucose medium or high glucose medium containing thapsigargin (0.25 μM). The

cells were allowed to grow for additional 24 or 48 hours before harvest for RNA or protein or subjected to Sulforhodamine B (SRB) or MTT assays.

Cell growth assay by Sulforhodamine B

Sulforhodamine B is a fluorescent dye which stains for the protein mass of culture cells and can be used as an indicator of cell growth or survival [25]. SRB was purchased from Sigma (St. Louis, MO, USA). Cancer cells were seeded into the 96-well plate in quadruplicate or triplicate at the density of 1000 cells per well. They were allowed to settle for 1 day, followed by 24 hours starvation in SFM with normal glucose and antibiotics. Then the cells were treated with high glucose, normal glucose, or thapsigargin (0.25 μM) in combination of normal glucose or high glucose. After incubation, 50 μl of 50% trichloroacetic acid (TCA) solution was added to each well to fix the cells and the 96-well plate was kept on ice for one hour. After fixation, the cells were washed 5 times with Milli-Q water and allowed for air dry. Dried plates were stained with 100 μl of 0.4% SRB in 1% acetic acid solution for 20 minutes. Stained cells were then washed 5 times with 1% acetic acid and excess liquid were removed. Then 100 μl of 25 mM Tris solution was added to each well and the plates were shaken mildly until all the SRB dissolved. The absorbance at 520 nm was measured using μQuant microplate reader from BioTek Instruments (Winooski, VT, USA).

Cell growth assay by MTT

Cell growth was determined by MTT assay [26]. MTT [3-(4,5-dimethylthiazol-2-yl)-2,5-diphenyltetrazolium bromide] was purchased from Sigma (St. Louis, MO, USA). The cancer cells were seeded into the 96-well plate in quadruplicate or triplicate at desired density (500 to 1000 cells/well) and allowed to settle for 24 hours, followed by 24 hours starvation in SFM with normal glucose (5.6 mM) and antibiotics. Then the cells were treated with high glucose, normal glucose, or thapsigargin (0.25 μM) in combination with normal glucose or high glucose. After treatment, the old medium was removed and replenished with fresh DMEM medium with normal glucose and 10% FBS plus antibiotics. Then 10 μl MTT solution (5 mg/ml in PBS) was added into the wells and incubated for 2 hours or until brown precipitates could be seen under microscope. The medium was then replaced with 100 μl DMSO, and the plate was shaken for 15 min and the absorbance at 570 nm was measured with μQuant microplate reader from BioTek Instruments (Winooski, VT, USA).

Cell growth assay by counting

HCT116 colorectal cancer cells were seeded into 24-well plates at the density of 10,000 cells per well and allowed to settle for 24 hours, followed by 24 hours starvation in SFM with normal glucose (5.6 mM) and antibiotics. Then the cells were treated with either high glucose or normal glucose in triplicates for each time point. At the end of each time point, the cells were trypsinized and counted to calculate the total numbers of cells in each well.

Flow cytometry analysis of cellular apoptosis

Cellular apoptosis was tested by flow cytometry after staining of apoptotic cells with FITC coupled annexin V and propidium iodide using the Dead cell apoptosis kit from Invitrogen (Cat No. V13242). After treatment with thapsigargin (0.25 μM) in normal glucose or high glucose medium, the cells were washed with PBS and then trypsinized. The collected cells were stained with FITC-annexin V and popidium iodide according to the standard protocol of the kit and analyzed with the BD FACSAria Fusion Cell Sorter.

Affymetrix microarray assay

We used the microarray approach to study the effects of high glucose treatment on gene expression in HCT116 colorectal cancer cells. RNA samples were harvested 24 hours after high glucose treatment. Cells grew in normal glucose and normal glucose plus mannitol were used as control. The RNA samples were analyzed in duplicates using the Affymetrix Human Gene 1.0 ST array (Affymetrix, Santa Clara, CA, USA). The experiments were carried out by the Li Ka Shing Institute of Health Sciences Core Laboratory according to the standard protocols of Affymetrix. GeneSpring v.11.5.1 was used for data analysis with quantile normalization to discover differentially expressed genes. The gene expression levels were compared using ANOVA for statistical

Table 1. List of primers for qPCR

Gene	Forward primer (5' to 3')	Reverse primer (5' to 3')
β-Actin	AGAGCTACGAGCTGCCTGAC	AGCACTGTGTTGGCGTACAG
Cyclin E2 (*CCNE2*)	TTGGCTATGCTGGAGGAAGT	CCTGGTGGTTTTTCAGTGCT
CDC25A	GAGATCGCCTGGGTAATGAA	TGCGGAACTTCTTCAGGTCT
STAT4	AGCCTTGCGAAGTTTCAAGA	ACACCGCATACACACTTGGA
MAT2A	AGGGATGCCCTAAAGGAGAA	CACAATGATTTTGCGTCCAG
CHOP (*DDIT3*)	GAGCGCCTGACCAGGGAAGT	GGCCCAAGTGGGGGACTGAT
TRIB3	GCCTCTGAACTGAGCCAAAC	AAGCAGGAACTGCATGTGTG
BiP (*HSPA5*)	TAGCGTATGGTGCTGCTGTC	TGACACCTCCCACAGTTTCA
ATF4	AGTGGCATCTGTATGAGCCCA	GCTCCTATTTGGAGAGCCCCT
VEGFA	AGGAGGAGGGCAGAATCATCA	CTCGATTGGATGGCAGTAGCT
XBP1 unspliced (variant 1)	TGCTGAGTCCGCAGCACTCA	GCTGGCAGGCTCTGGGGAAG
XBP1 spliced (variant 2)	TGCTGAGTCCGCAGCAGGTG	GCTGGCAGGCTCTGGGGAAG

analysis. Genes with 50% increase or decrease in expression levels between the normal glucose and high glucose groups and a significant *P* value (P<0.05) were selected for pathway analysis and gene enrichment analysis.

RNA extraction and quantitative real-time PCR

RNA was extracted from the treated cancer cells using the Trizol reagent from Invitrogen. All procedures were carried out with the standard protocols provided by the manufacturer. The RNA had good quality with an A260/A280 ratio over 1.9. Gene expression changes detected by microarray were validated by quantitative real-time PCR (qPCR) using the SYBR Green method. First strand cDNA was synthesized by the High-Capacity cDNA Reverse Transcription Kit from ABI Biosystems (Foster City, CA, USA) using 0.3 μg total RNA as template. The SYBR Green method was used for qPCR detected by an ABI ViiA 7 Real-time PCR system and SYBP® Premix Ex Taq™ (Perfect Real Time) from Takara (Mountain View, CA, USA). The expression levels of each tested gene were validated by qPCR for 40 cycles. The expression levels were normalized to the expression level of β-actin. **Table 1** lists the primers used for these experiments.

Western blot analysis for protein expression

Changes in protein levels were tested by Western blot analysis. The antibodies for CHOP (#5554), cyclin E2 (#4132), BiP (#3177), ATF4 (11815), XBP-1s (12782), β-actin (#4967) and cleaved caspase-3 (#9661) were purchased from Cell Signaling Technology. After treatments, cells were lysed with lysis buffer containing 0.15 M NaCl, 0.05 M Tris-HCl (pH 7.4), 0.5% sodium deoxycholate, 1% NP-40, 0.1% Triton X-100, 1 mM EDTA, 1 mM EGTA plus Complete protease inhibitor cocktail. Protein concentrations were measured by the BCA Protein Assay Kit (Thermo Fisher Scientific). The protein extracts were separated on 10% or 15% SDS-PAGE gels and transferred to polyvinylidine difluoride (PVDF) membranes. After transfer, the PVDF membranes were blocked in 5% non-fat milk in 0.15 M NaCl, 0.05 M Tris-HCl (pH 7.4) with 0.1% Tween-20 (TBST). Then the PVDF membranes were cut into strips for overnight incubation at 4°C with different primary antibodies diluted in 5% non-fat milk in TBST. With this setting, one membrane can be incubated with multiple primary antibodies simultaneously according to the different sizes of the targets. After washes in TBST, the membranes were incubated for 1 hour at room temperature with horseradish peroxidase-conjugated secondary antibody (1:2,000, Abcam, Cambridge, MA). After incubation with secondary antibodies, the membranes were washed three times with TBST and the protein bands were visualized using Amersham ECL chemiluminescence detection reagent from GE Healthcare (Piscataway, NJ, USA) with the Bio-Rad ChemiDoc MP imaging system or using X-Ray film.

Results

The legacy effects of high glucose on HCT116 cell growth

We tested the effects of high glucose on HCT116 cell growth using the MTT and SRB

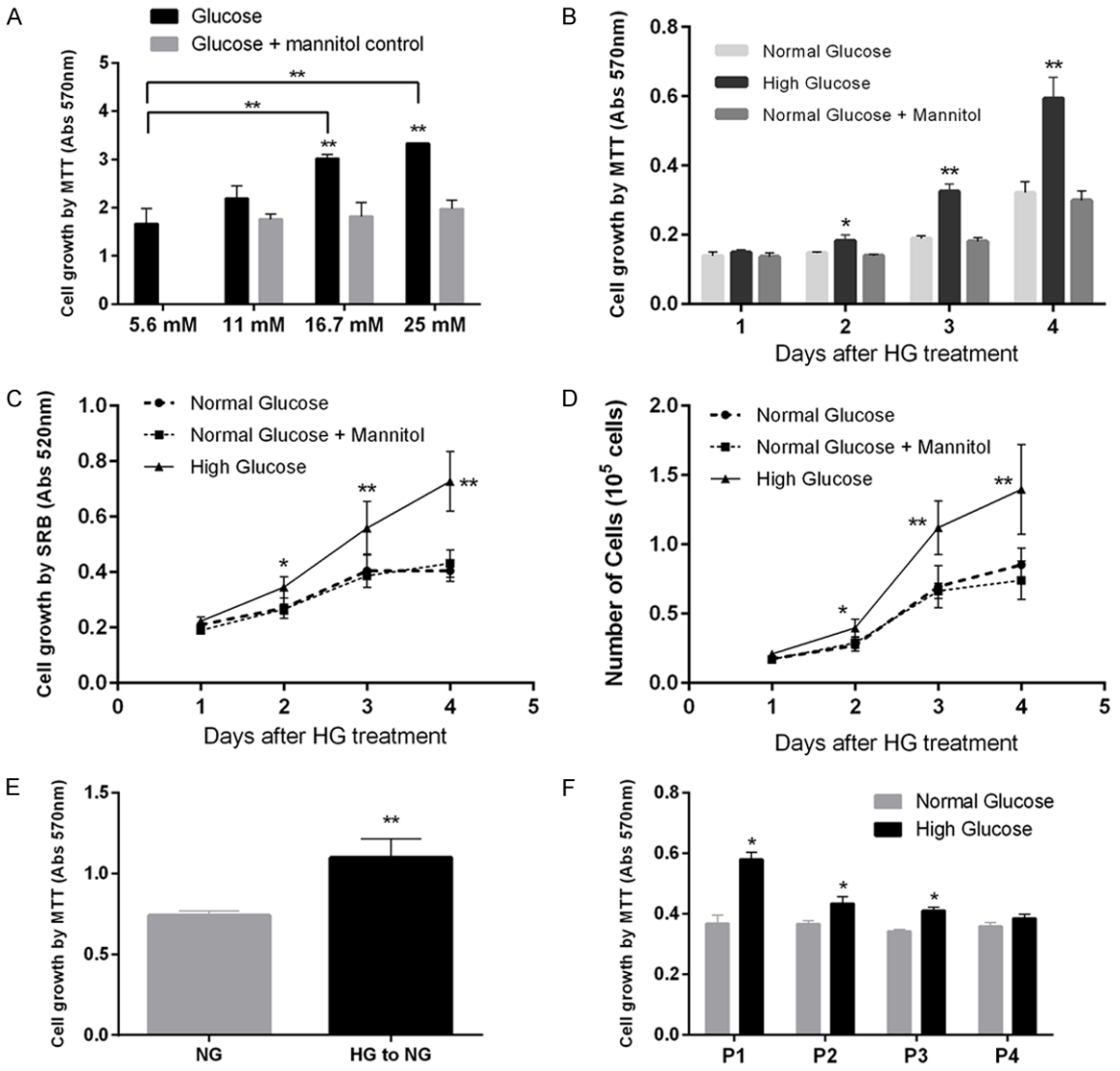

Figure 1. Effect of high glucose on growth of HCT116 colon cancer cells. (A) HCT116 colon cancer cells were grown in DMEM with different concentrations of glucose or glucose plus mannitol for 48 hours and then measured by MTT assay. To control for the change of osmolality, mannitol was added to the amount equal to the additional glucose added (5.4 mM for 11 mM glucose, 11.1 mM for 16.7 mM glucose and 19.4 mM for 25 mM glucose). (B and C) Time course of HCT116 cell growth in high glucose (25 mM) with cells in normal glucose and normal glucose plus mannitol as control using the MTT assay (B) and SRB assay (C). (D) HCT116 cell growth in 25 mM high glucose medium determined by cell counting using cells in normal glucose and normal glucose plus mannitol as controls. (E) HCT116 cells maintained in high glucose were plated out in normal glucose (HG to NG) and grown for two days and then measured by MTT assay with HCT116 cells in normal glucose (NG) as control. (F) High glucose maintained HCT116 cells were switched to grow in normal glucose medium and kept for successive passages. P1 refers to one additional passage. The cells were kept until 4 passages (P4). MTT assays were performed 2 days after plating out of the cells. For all the experiments, the MTT and SRB assays were performed in quadruplicates (n=4) or triplicates (n=3) and repeated. The cell counting experiments were performed in triplicates (n=3). The graphs shown were one of the representative experiments in bar charts (mean ± SD). $^{*}0.01\leq P<0.05$, $^{**}P<0.01$.

assays. HCT116 colorectal cancer cells were grown in different concentrations of glucose for 48 hours. To control for the change of osmolality, mannitol was added to the amount equal to the additional glucose added. The growth of HCT116 cell increased with increasing glucose concentration up to 25 mM reaching significance for 16.7 mM and 25 mM when compared with normal glucose (**Figure 1A**). We further tested the time course of the growth promotion

in high glucose with 25 mM glucose treatment. The growth of HCT116 cells showed no significant difference in the first 24 hours but showed significant growth increase in high glucose from the second day to 4 days in the high glucose environment (**Figure 1B**). SRB is a dye that can bind to the protein mass of culture cells and serves as an indicator of cell growth [25]. We used SRB assay to show that high glucose condition increased cell growth of HCT116 cells from day 2 to day 4 after switch to the high glucose medium (**Figure 1C**). Additionally, cell counting corroborated the significant increase in cell number in high glucose environment from day 2 to day 4 (**Figure 1D**).

We then asked the question if exposure to high glucose had legacy effects on HCT116 cell growth when the cells were switched back to normal glucose medium. We used HCT116 cells that had been maintained in high glucose medium and switched back to normal glucose medium. We observed significant increase in cell growth with MTT (**Figure 1E**) assay although the magnitude of increase was less than the difference between the changes in normal versus high glucose medium. We kept the high glucose exposed cells in normal glucose medium for additional passages and observed significant increase in cell growth up to three passages (P3) with decreasing magnitude of increment for each successive passage (**Figure 1F**).

The effects of high glucose on gene expression change in HCT116 cells

We used the microarray approach to study the effect of high glucose treatment on gene expression. With the Affymetrix Human Gene 1.0 ST microarray, expression of over 28,000 genes was detected. The result was analyzed using GeneSpring software. Using ANOVA for comparison of the expression among normal glucose-, high glucose- and normal glucose plus mannitol-treated HCT116 cells, 3520 probe clusters showed significant differences in gene expression and 100 of them showed greater than 50% change in gene expression. **Table 2** summarized the probe clusters that showed significant changes, 58 of them showed increased expression and 42 showed decreased expression (**Table 2**).

We used DAVID (http://david.abcc.ncifcrf.gov/home.jsp) to examine for pathway enrichment for these differentially expressed genes. **Table 3** summarized the enriched pathways affected by high glucose treatment in HCT116 cells. The pathways were mainly implicated in stress response, DNA replication, apoptosis, ER stress and regulation of programmed cell death. Reduced expression was mainly found in genes whose products were located in the ER or related to its function.

Validation of gene expression changes by quantitative real-time PCR (qPCR)

The genes which showed increased expression in high glucose were mainly related to promotion of cell proliferation (*STAT4*, *CDC25A* and *MAT2A*) and progression of cell cycle (*CCNE2*). We used qPCR to test the expression of these genes in HCT116 cells in high glucose medium and validated the increased gene expression (**Figure 2A**). We also used qPCR to confirm the reduced expression of CHOP (gene symbol *DDIT3*), BiP (gene symbol *HSPA5*) and *TRIB3* in HCT116 cells in high glucose medium (**Figure 2A**). Using Western blot assays, we confirmed the increase in protein level of STAT4 and Cycline E2 (*CCNE2*) and decrease in protein levels of BiP and CHOP in HCT116 cells in high glucose medium (**Figure 2B**).

HCT116 colon cancer cells exposed to high glucose are more resistant to ER stress induced by thapsigargin

HCT116 colon cancer cells showed decreased expression of genes whose products are located in the ER or in the ER stress pathway. We used thapsigargin to induce ER stress in HCT116 colon cancer cells. Thapsigargin is an inhibitor of the ER specific calcium ATPase with potential anti-cancer function. It blocks the calcium influx to the ER and stops the ER from executing its normal function [27]. We used different concentrations of thapsigarain to treat HCT116 cells (0.01-1 μM) in normal and high glucose medium for 2 days. In low concentration of thapsigargin (0.01 μM), there were minimal inhibition of HCT116 cell growth in both normal and high glucose medium. When treated with 1 μM of thapsigargin, the growth inhibition in normal glucose medium was more prominent when compared to high glucose medium on day 1 (**Figure 3A**). By day 2, the growth inhibition was almost complete in both normal and high glucose condition although at lower concentration thapsigargin,

Table 2. Summary of gene expression changes in HCT116 cells after 24-hour high glucose treatment

Transcript cluster ID	NG	NG + Mannitol	HG	Fold change	*P* (ANOVA)	*P* (HG vs. NG)	Gene symbol	Description
7900336	9.07	9.22	8.13	-1.915	0.0007	0.0001	MACF1	microtubule-actin crosslinking factor 1
7901054	9.36	9.45	8.77	-1.506	0.0078	0.0025	PLK3	polo-like kinase 3 (Drosophila)
7902512	9.25	9.29	9.93	1.594	0.0227	0.0150	DNAJB4	DnaJ (Hsp40) homolog, subfamily B, member 4
7904953	6.77	6.59	7.64	1.818	0.0208	0.0161		
7914851	8.18	8.22	8.90	1.649	0.0031	0.0193	CLSPN	claspin homolog (Xenopus laevis)
7914878	8.53	8.46	9.15	1.539	0.0045	0.0087	LOC100289612	arsenic transactivated protein 1
7917728	8.40	8.54	8.99	1.512	0.0306	0.0084	FAM69A	family with sequence similarity 69, member A
7920877	9.77	9.77	9.11	-1.583	0.0096	0.0023	ARHGEF2	Rho/Rac guanine nucleotide exchange factor (GEF) 2
7922337	8.00	8.13	7.22	-1.718	0.0153	0.0019	TNFSF18	tumor necrosis factor (ligand) superfamily, member 18
7922846	8.50	8.38	7.69	-1.748	0.0025	0.0021	FAM129A	family with sequence similarity 129, member A
7923173	8.50	8.59	7.68	-1.766	0.0231	0.0054	MIR181B1	microRNA 181b-1
7925500	8.30	8.13	8.99	1.615	0.0177	0.0448	CHML	choroideremia-like (Rab escort protein 2)
7926259	9.55	9.49	10.16	1.522	0.0369	0.0239	MCM10	minichromosome maintenance complex component 10
7930413	11.30	11.56	10.61	-1.620	0.0004	0.0084	DUSP5	dual specificity phosphatase 5
7938485	9.12	8.99	8.50	-1.538	0.0013	0.0001	MICAL2	microtubule associated monoxygenase, calponin and LIM domain containing 2
7940147	8.65	8.77	9.69	2.054	0.0486	0.0256	FAM111B	family with sequence similarity 111, member B
7942839	9.44	9.57	10.11	1.590	0.0031	0.0009	PCF11	PCF11 cleavage and polyadenylation factor subunit
7949383	10.26	9.84	9.43	-1.779	0.0352	0.0141	SYVN1	synovial apoptosis inhibitor 1
7949836	9.67	9.27	8.71	-1.941	0.0173	0.0218	CDK2AP2	cyclin-dependent kinase 2 associated protein 2
7952145	11.03	10.66	9.97	-2.078	0.0466	0.0230	HYOU1	hypoxia up-regulated 1
7952673	6.77	7.22	7.60	1.773	0.0026	0.0039	FLJ45950	
7954398	6.43	6.38	5.72	-1.633	0.0080	0.0038	C12orf39	chromosome 12 open reading frame 39
7957126	8.42	8.27	9.01	1.506	0.0119	0.0109	KCNMB4	potassium large conductance calcium-activated channel, subfamily M, beta member 4
7960544	8.28	8.36	8.88	1.511	0.0164	0.0194	VAMP1	vesicle-associated membrane protein 1 (synaptobrevin 1)
7964460	9.46	9.24	7.31	-4.464	0.0014	0.0002	DDIT3	DNA-damage-inducible transcript 3, CHOP
7964834	6.59	6.58	7.57	1.971	0.0021	0.0010	CPM	carboxypeptidase M
7986350	6.45	6.37	7.30	1.806	0.0058	0.0024	ARRDC4	arrestin domain containing 4
7989307	6.97	6.89	6.30	-1.591	0.0049	0.0046		
7989657	8.13	8.07	8.96	1.778	0.0313	0.0335	CSNK1G1	casein kinase 1, gamma 1
7995354	8.61	8.76	9.26	1.564	0.0104	0.0055	ORC6L	origin recognition complex, subunit 6 like (yeast)
7998927	6.79	6.89	7.72	1.906	0.0047	0.0061		
8016832	8.58	8.67	9.44	1.814	0.0042	0.0030	MMD	monocyte to macrophage differentiation-associated
8017850	10.87	10.57	10.00	-1.826	0.0335	0.0113	WIPI1	WD repeat domain, phosphoinositide interacting 1
8020164	7.94	7.91	8.56	1.535	0.0035	0.0033	GNAL	guanine nucleotide binding protein (G protein)
8026106	12.30	12.09	11.69	-1.522	0.0421	0.0195	CALR	calreticulin
8027002	12.74	13.06	11.55	-2.287	0.0065	0.0052	GDF15	growth differentiation factor 15
8027297	8.55	8.47	9.45	1.867	0.0001	0.0042	ZNF738	zinc finger protein 738

8035445	9.79	10.04	9.20	-1.502	0.0186	0.0219	JUND	jun D proto-oncogene
8035838	9.11	9.25	9.73	1.540	0.0114	0.0040	ZNF724P	zinc finger protein 724 (pseudogene)
8041179	9.47	9.83	8.80	-1.589	0.0050	0.0049	CLIP4	CAP-GLY domain containing linker protein family, member 4
8042503	9.21	9.50	8.42	-1.726	0.0018	0.0010	MXD1	MAX dimerization protein 1
8043187	12.22	12.04	12.88	1.573	0.0077	0.0118	MAT2A	methionine adenosyltransferase II, alpha
8043995	7.22	6.81	7.81	1.506	0.0109	0.0031	IL1R1	interleukin 1 receptor, type 1
8046003	7.47	7.45	8.62	2.218	0.0023	0.0003	GCA	grancalcin, EF-hand calcium binding protein
8049961	10.80	10.86	10.09	-1.631	0.0122	0.0119	FBXO25	F-box protein 25|hypothetical LOC728323
8053737	7.56	7.69	8.24	1.605	0.0023	0.0019	ANKRD20B	ankyrin repeat domain 20B
8054377	9.88	9.95	9.24	-1.558	0.0033	0.0038	FHL2	four and a half LIM domains 2
8055952	9.79	9.85	9.16	-1.544	0.0184	0.0091	NR4A2	nuclear receptor subfamily 4, group A, member 2
8056285	7.41	7.37	8.05	1.563	0.0291	0.0147	IFIH1	interferon induced with helicase C domain 1
8057771	6.54	6.47	7.17	1.546	0.0167	0.0011	STAT4	signal transducer and activator of transcription 4
8059177	10.11	10.02	10.69	1.503	0.0029	0.0067	TUBA4A	tubulin, alpha 4a
8060344	10.00	9.93	8.67	-2.510	0.0315	0.0129	TRIB3	tribbles homolog 3 (Drosophila)
8060835	6.66	6.66	7.36	1.621	0.0019	0.0223		
8074853	6.59	6.65	7.19	1.524	0.0271	0.0042	ZNF280A	zinc finger protein 280A
8077712	8.13	7.83	7.30	-1.777	0.0200	0.0182	CRELD1	cysteine-rich with EGF-like domains 1
8081758	7.33	7.39	7.95	1.538	0.0455	0.0235	GRAMD1C	GRAM domain containing 1C
8083282	10.19	10.05	10.80	1.522	0.0011	0.0048	HPS3	Hermansky-Pudlak syndrome 3
8084634	11.55	11.26	10.68	-1.837	0.0420	0.0097	DNAJB11	DnaJ (Hsp40) homolog, subfamily B, member 11
8086880	8.41	8.25	9.01	1.512	0.0051	0.0091	CDC25A	cell division cycle 25 homolog A (S. pombe)
8096917	7.05	7.34	6.40	-1.562	0.0346	0.0203		
8098103	7.59	7.59	8.24	1.569	0.0076	0.0057	FNIP2	folliculin interacting protein 2
8103695	7.21	7.28	7.83	1.538	0.0212	0.0013	MFAP3L	microfibrillar-associated protein 3-like
8104570	7.64	7.74	8.26	1.531	0.0256	0.0073	FAM105A	family with sequence similarity 105, member A
8107194	8.52	8.48	9.13	1.523	0.0053	0.0138	C5orf30	chromosome 5 open reading frame 30
8113491	10.06	10.12	9.09	-1.954	0.0185	0.0007	STARD4	StAR-related lipid transfer (START) domain containing 4
8117594	11.87	11.58	12.68	1.753	0.0113	0.0361	HIST1H2BM	histone cluster 1, H2bm
8118310	10.19	10.18	11.09	1.862	0.0146	0.0129	HSPA1A HSPA1B	heat shock 70 kDa protein 1A heat shock 70 kDa protein 1B
8118314	10.02	10.03	10.99	1.968	0.0114	0.0139	HSPA1B HSPA1A	heat shock 70 kDa protein 1B heat shock 70 kDa protein 1A
8119898	10.53	10.73	9.91	-1.528	0.0074	0.0119	VEGFA	vascular endothelial growth factor A
8119918	7.69	7.67	6.96	-1.655	0.0079	0.0120	C6orf223	chromosome 6 open reading frame 223
8121002	8.79	8.65	9.47	1.596	0.0051	0.0097	C6orf162	chromosome 6 open reading frame 162
8122816	9.66	9.45	8.94	-1.650	0.0402	0.0180		
8123609	9.40	9.42	10.08	1.602	0.0120	0.0070	SERPINB9	serpin peptidase inhibitor, clade B (ovalbumin), member 9
8126629	10.03	9.93	9.37	-1.581	0.0164	0.0084	GTPBP2	GTP binding protein 2
8127346	8.69	8.90	9.40	1.644	0.0126	0.0062	RAB23	RAB23, member RAS oncogene family
8128606	7.53	7.35	8.15	1.536	0.0015	0.0030	RTN4IP1	reticulon 4 interacting protein 1
8135069	8.42	8.59	7.83	-1.508	0.0106	0.0155	SERPINE1	serpin peptidase inhibitor, clade E (nexin, plasminogen activator inhibitor type 1), member 1
8135392	9.41	9.60	8.81	-1.519	0.0075	0.0038	HBP1	HMG-box transcription factor 1

8135514	9.28	9.41	8.66	-1.535	0.0137	0.0038	IFRD1	interferon-related developmental regulator 1
8137783	8.63	8.66	8.03	-1.508	0.0019	0.0064	TMEM184A	transmembrane protein 184A
8139832	7.45	7.68	8.12	1.590	0.0166	0.0067	ZNF117	zinc finger protein 117
8143684	12.08	11.75	11.24	-1.789	0.0283	0.0148	PDIA4	protein disulfide isomerase family A, member 4
8145122	11.69	11.55	11.11	-1.502	0.0087	0.0025	SLC39A14	solute carrier family 39 (zinc transporter), member 14
8146130	8.44	8.42	9.03	1.503	0.0060	0.0038	GINS4	GINS complex subunit 4 (Sld5 homolog)
8151042	7.18	7.09	7.83	1.567	0.0171	0.0046	TTPA	tocopherol (alpha) transfer protein
8151871	9.06	8.94	10.05	1.986	0.0241	0.0227	CCNE2	cyclin E2
8154381	9.80	10.07	7.99	-3.515	0.0026	0.0026	C9orf150	chromosome 9 open reading frame 150
8155414	7.97	8.06	8.72	1.680	0.0002	0.0039	ANKRD20B	ankyrin repeat domain 20B
8155574	7.66	7.68	8.25	1.502	0.0101	0.0063	ANKRD20A1	ankyrin repeat domain 20 family, member A1
8155591	8.42	8.50	9.08	1.579	0.0034	0.0025	ANKRD20B	ankyrin repeat domain 20B
8155602	7.79	7.84	8.41	1.528	0.0058	0.0021	ANKRD20A2	ankyrin repeat domain 20 family, member A2
8160431	7.86	8.18	7.08	-1.719	0.0016	0.0076	LOC554202	
8161384	7.97	8.06	8.72	1.686	0.0002	0.0039	CCDC29	coiled-coil domain containing 29
8161415	8.20	8.44	8.80	1.520	0.0026	0.0101	CCDC29	coiled-coil domain containing 29
8164165	13.54	13.16	12.40	-2.208	0.0396	0.0148	HSPA5	heat shock 70 kDa protein 5 (glucose-regulated protein, 78 kDa), BiP
8167910	5.33	5.58	6.16	1.766	0.0074	0.0043		
8172268	8.65	8.53	8.02	-1.556	0.0068	0.0038	MIR222	microRNA 222
8178086	9.99	10.01	10.96	1.956	0.0140	0.0146	HSPA1B HSPA1A	heat shock 70 kDa protein 1B heat shock 70 kDa protein 1A
8179322	10.05	10.04	10.94	1.848	0.0159	0.0136	HSPA1A HSPA1B	heat shock 70 kDa protein 1A heat shock 70 kDa protein 1B
8179324	9.99	10.01	10.96	1.956	0.0138	0.0146	HSPA1B HSPA1A	heat shock 70 kDa protein 1B heat shock 70 kDa protein 1A

The table is arranged by probe cluster ID from Affymetrix. The expression levels of NG-, NG + mannitol- and HG-treated HCT116 cells were in log2 scale. The values are the mean of duplicate samples. The *P* values for ANOVA three-way comparison were listed. The comparison of HG vs. NG was from unpaired t test.

Table 3. Enriched pathways for differentially expressed genes after high glucose treatment

Term	Count	Gene List	*P* value	Bonferroni *P*	Benjamini *P*
Genes with increased expression					
GO:0006270~DNA replication initiation	4	*MCM10, ORC6, GINS4, CCNE2*	3.30e-05	0.0055	0.0055
GO:0006260~DNA replication	5	*CLSPN, MCM10, ORC6, CDC25A, GINS4*	2.32e-04	0.0380	0.0192
Genes with decreased expression					
hsa04141: Protein processing in endoplasmic reticulum	7	*SYVN1, HYOU1, DDIT3* (CHOP), *CALR, DNAJB11, PDIA4, HSPA5* (BiP)	1.94e-06	6.98e-05	6.98e-05
GO:0036498~IRE1-mediated unfolded protein response	5	*SYVN1, HYOU1, WIPI1, HSPA5* (BiP), *DNAJB11*	3.52e-06	0.0014	0.0014
GO:0005790~smooth endoplasmic reticulum	4	*SYVN1, HYOU1, CALR, HSPA5* (BiP)	1.13e-05	0.0010	0.0010
GO:0000122~negative regulation of transcription from RNA polymerase II promoter	9	*PLK3, DDIT3* (CHOP), *CALR, JUND, MXD1, FHL1, NR4A2, TRIB3, VEGFA*	2.78e-05	0.0108	0.0036
GO:0034663~endoplasmic reticulum chaperone complex	3	*HYOU1, DNAJB11, HSPA5* (BiP)	1.53e-04	0.0141	0.0071
short sequence motif: Prevents secretion from ER	4	*HYOU1, CALR, PDIA4, HSPA5* (BiP)	1.63e-04	0.0207	0.0207
GO:0005788~endoplasmic reticulum lumen	5	*HYOU1, CALR, DNAJB11, PDIA4, HSPA5* (BiP)	3.01e-04	0.0276	0.0093
GO:0051087~chaperone binding	4	*SYVN1, HYOU1, CALR, HSPA5* (BiP)	4.34e-04	0.0487	0.0487

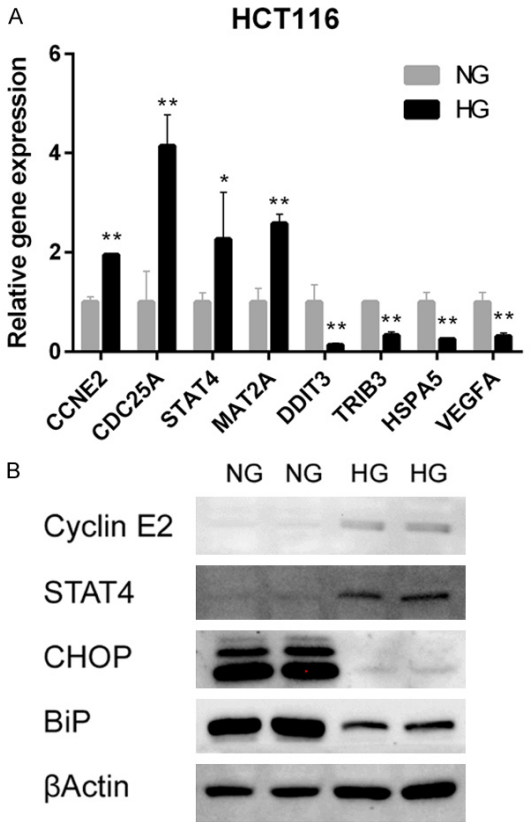

Figure 2. Validation of gene expression change by qPCR and Western blot analysis. A: Expressions of selected genes from the microarray study were validated by qPCR. The bar charts represent mean ± SD. NG, cells in normal glucose medium; HG, cells treated with high glucose medium. For the qPCR validations, the experiment was in duplicates (n=2) and repeated with one of the representative experiment shown. $^{*}0.01\leq P<0.05$ NG vs. HG, $^{**}P<0.01$ NG vs. HG. B: Western blot analysis to show the changes in protein levels of BiP (*HSPA5*), CHOP (*DDIT3*), Cyclin E2 (*CCNE2*) and STAT4 with βActin as internal control in HCT116 cells grown in high glucose (HG) or normal glucose (NG) media for 2 days. The experiment was repeated and one of the representative results was shown.

cells exposed to high glucose showed more resistance to the growth inhibition than those exposed to normal glucose (**Figure 3B**). Since exposure to high glucose suggested legacy effect with persistence of growth of HCT116 colon cancer cells when switched from high glucose medium to normal glucose medium, we further tested the effect of thapsigargin in altering this legacy effect. Upon transfer from high glucose to normal glucose medium, using MTT (**Figure 3C**) and SRB (**Figure 3D**) assays, we confirmed that high glucose conditioned HCT116 cells showed attenuated growth inhibition by thapsigargin versus those maintained in normal glucose without prior exposure to high glucose.

ER stress genes are activated in thapsigargin-treated HCT116 cells

The UPR is a self-saving mechanism for the cell during ER stress. Dysfunctional ER can lead to increased accumulation of unfolded proteins or proteins with abnormal three dimensional structures. These proteins can form aggregates inside the cell and trigger cell death. As a chaperone protein, BiP is released from its binding proteins including PERK, IRE1 and ATF6 in order to stabilize these abnormal proteins. The uncoupling of these proteins trigger the UPR with activation of transcription factors and increased production of chaperon proteins [20]. In thapsigargin-treated HCT116 colon cancer cells under normal and high glucose condition, the transcription factor, *ATF4,* was activated to increase expression of BiP (**Figure 4A** and **4B**). Western blot analysis confirmed increased expression of ATF4 and BiP protein in thapsigargin treated HCT116 cells in high glucose condition (**Figure 4E**).

In the ER stress condition, release of IRE1 from its binding with BiP and the activation of IRE1 will lead to splicing of XBP-1 mRNA to generate the spliced forms of XBP-1, XBP-1 variant 2 (XBP1 v2). The spliced form of XBP-1 mRNA is then translated to produce the transcription factor XBP-1s which activates genes implicated in ER stress. We used specific primers to detect different forms of XBP-1 using qPCR (**Table 1**).

Without thapsigargin treatment, there were low expression of unspliced XBP-1 mRNA (XBP1 v1) and its spliced form in the HCT116 colon cancer cells (**Figure 4C** and **4D**). When thapsigargin was added, the expression of spliced XBP-1 was increased in both normal and high glucose condition. In high glucose condition, the majority of the XBP-1 was expressed in the spliced form, suggesting a more robust response to ER stress in the high glucose condition. Using Western blot analysis, we showed activated protein levels of XBP-1s in thapsigargin-treated HCT116 cells in normal and high glucose condition but the activation was higher in the high glucose condition.

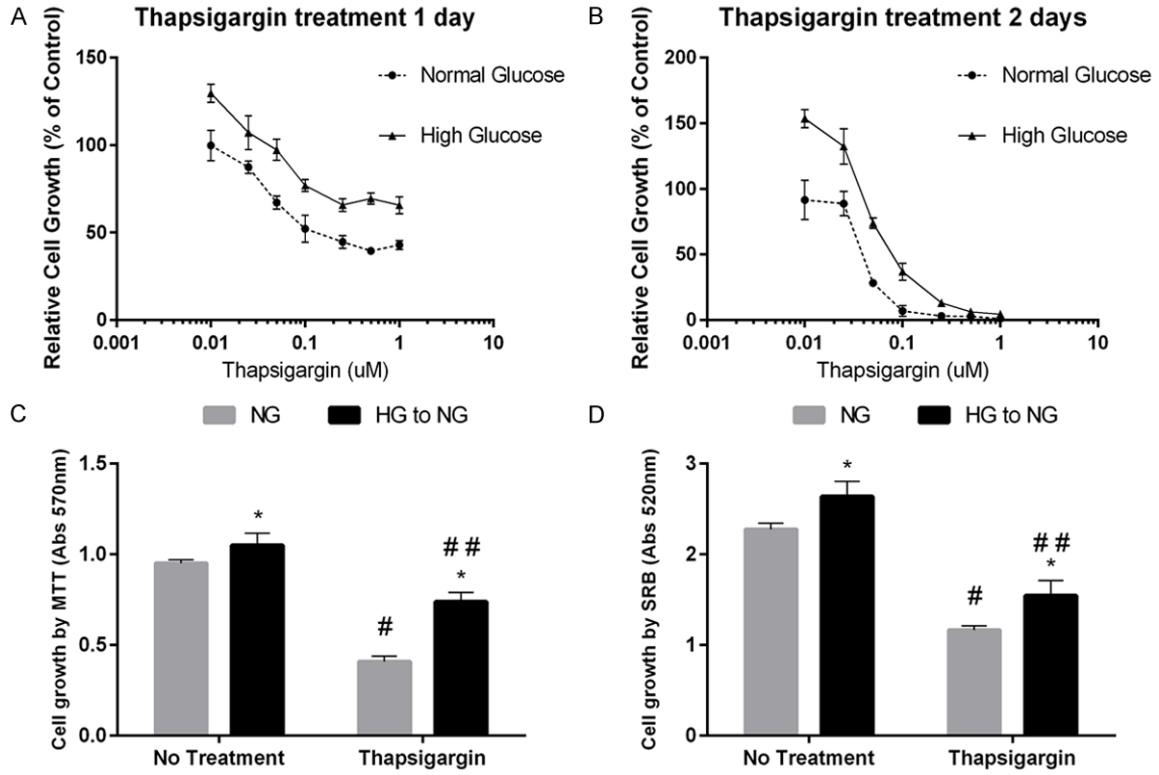

Figure 3. Effect of thapsigargin on HCT116 cell growth. (A and B) Dose effect of thapsigargin on HCT116 cells growth in normal glucose or high glucose media for 1 day (A) or 2 days (B). Cell viability was measured by MTT at the specified time after thapsigargin addition. Untreated cells in normal glucose or high glucose media were used as control. (C and D) HCT116 cells previously maintained in high glucose medium were plated out in normal glucose medium (HG to NG) and allowed to grow for 1 day. HCT116 cells in normal glucose medium (NG) were used as control. One day after plating out the cells, 0.25 μM thapsigargin was added and the cells were allowed to grow for one more day before MTT (C) or SRB (D) assays to measure the cell growth. The experiments were performed in quadruplicates (n=4) and repeated. The graphs shown were one of the representative experiments in bar charts (mean ± SD), *P<0.05 NG vs. HG to NG, #P<0.05 NG + thapsigargin vs. NG only, ##P<0.05 HG to NG + thapsigargin vs. HG to NG only.

HCT116 colon cancer cells exposed to high glucose are more resistant to apoptosis in ER stress

The ER-stress activated CHOP is a transcription factor, which regulates the expression of several genes that can lead to apoptosis and cell death in ER stress. TRIB3, a kinase regulated by CHOP, sensitizes cells to TNF- and TRAIL-induced apoptosis and negatively regulates NFκB [28]. As a downstream gene regulated by CHOP, TRIB3 mRNA was increased by thapsigargin treatment but its level was lower in high glucose as compared with normal glucose condition (**Figure 5A**). In light of these different responses of TRIB3, we tested the level of cleaved caspase-3 which is a downstream executor of apoptosis [29, 30]. Once caspase-3 is cleaved and activated, it represents an irreversible step of apoptosis. Using Western blot analysis, we confirmed reduced cleaved caspase-3 in high glucose condition when treated with thapsigargin (**Figure 5B**). Cyclin E2, an activator of cell cycle progression, showed lower RNA (**Figure 5A**) and protein levels (**Figure 5B**) in thapsigargin-treated HCT116 cells in both normal and high glucose conditions. BiP expression was activated by thapsigargin treatment and even higher in high glucose condition (**Figure 5**), but its protein levels showed activation only in thapsigargin-treated HCT116 cells with no difference between normal and high glucose conditions (**Figure 5B**).

We also used annexin V staining and flow cytometry analysis to visualize the apoptotic and necrotic cells because annexin V binds

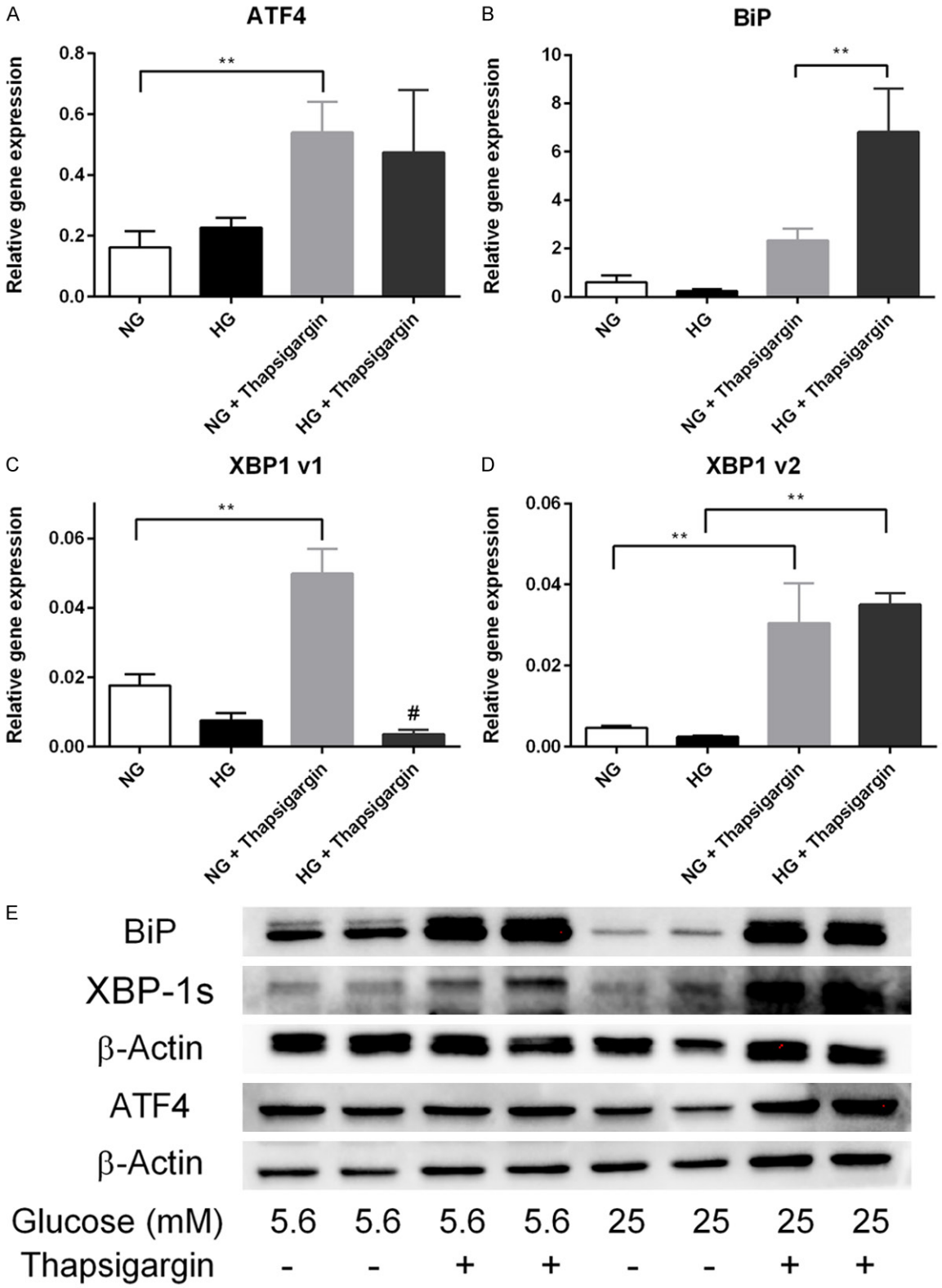

Figure 4. Effect of thapsigargin treatment on expression of ER stress genes. Expression of selected ER stress genes were tested by qPCR using the expression of β-actin as internal control for normalization. The bar charts represent mean ± SD. (A) ATF4, (B) BiP, (C) XBP-1 unspliced (variant 1), (D) XBP-1 spliced (variant 2), (E) Western blot results showing the protein levels of selected genes in thapsigargin-treated HCT116 cells in normal and high glucose media. β-Actin at third panel from top was the loading control for BiP and XBP1-s and β-Actin at bottom panel was the loading control for ATF4. **P<0.01, NG + thapsigargin vs. HG + thapsigargin. The qPCR experiment was repeated in duplicates (n=2) and one of the representative experiments was shown.

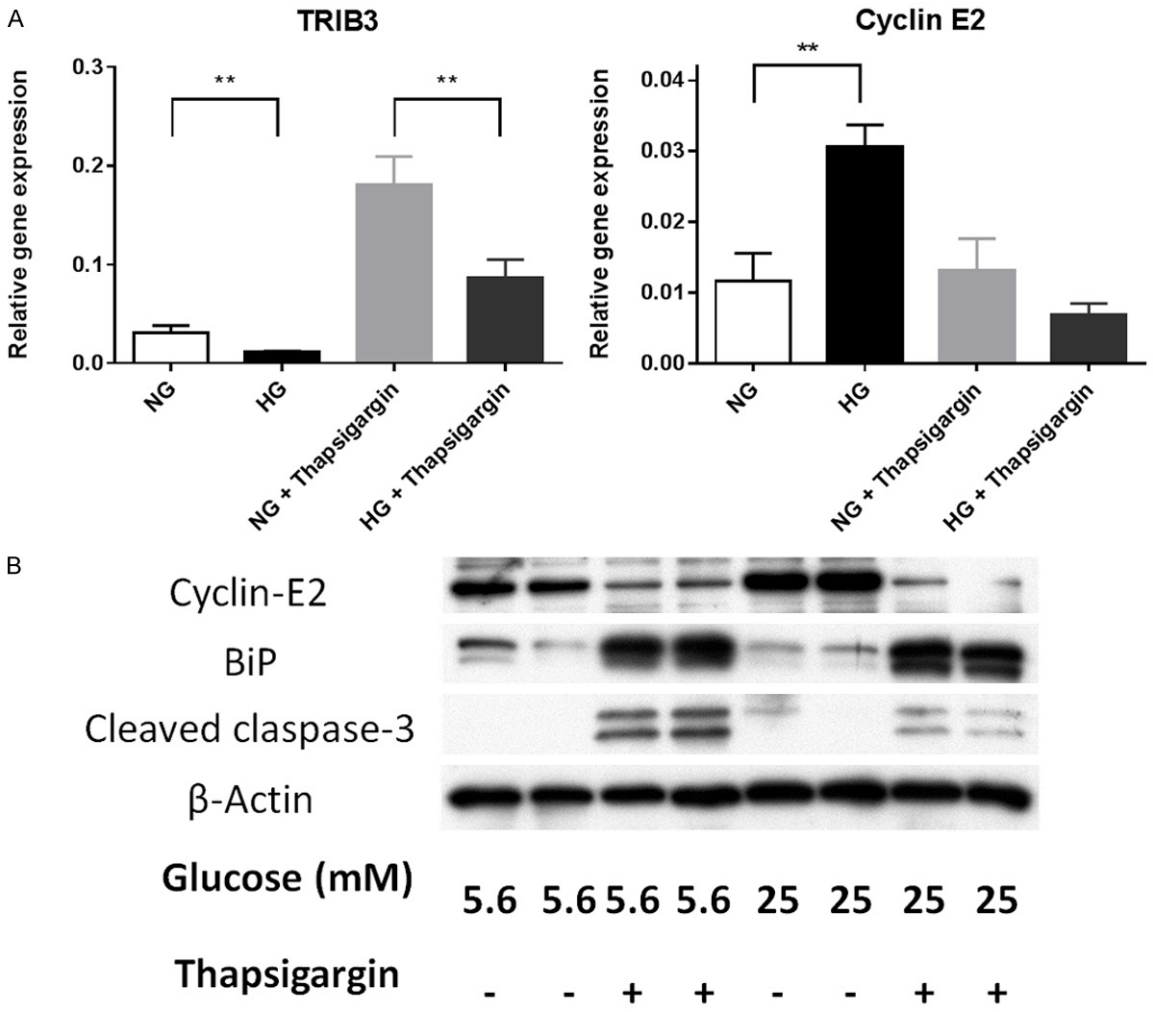

Figure 5. Cell growth and apoptosis of thapsigargin-treated HCT116 cells. A: Expression of TRIB3 and cyclin E2 (*CCNE2*) in thapsigargin-treated HCT116 cells in normal and high glucose conditions were tested by qPCR using the expression of β-actin as internal control for normalization. The experiment was done twice in duplicates (n=2) and one of the representative experiments was shown. The bar charts represent mean ± SD. $^{**}P<0.01$. B: The protein levels of cyclin E2, BiP and cleaved caspase-3 were tested by Western blot analysis. The expression level of β-actin was used as internal control. The Western blots were from the same gel. The Western blot experiment was repeated and one of the representative results was shown.

the exposed phosphatidylserine on the outer plasma membrane of apoptotic cells [31]. HCT116 cells treated with thapsigargin in normal glucose medium showed more annexin V positive and popidium iodide positive cells than treated cells exposed to high glucose medium (**Figure 6**). These findings indicated that thapsigargin treatment induced more apoptosis in HCT116 cells in normal glucose medium while HCT116 cells exposed to high glucose were more resistant to apoptotic effects of thapsigargin. **Table 4** summarizes the overall effects of thapsigargin in HCT116 cells treated in normal glucose and cells conditioned in high glucose medium.

Discussion

Cancer growth is characterized by increased cellular protein synthesis. For the first time, we reported the adaptability of UPR under ER stress which promoted survival of cancer cells exposed to high glucose condition and their resistance to apoptosis induced by anti-cancer prodrugs, such as thapsigargin, which utilizes the ER pathway to induce cancer cell death. These effects persisted despite returning the cells to normal glucose condition, indicating a legacy effect of transient high glucose exposure on cancer cell proliferation. These findings are clinically relevant suggesting that control-

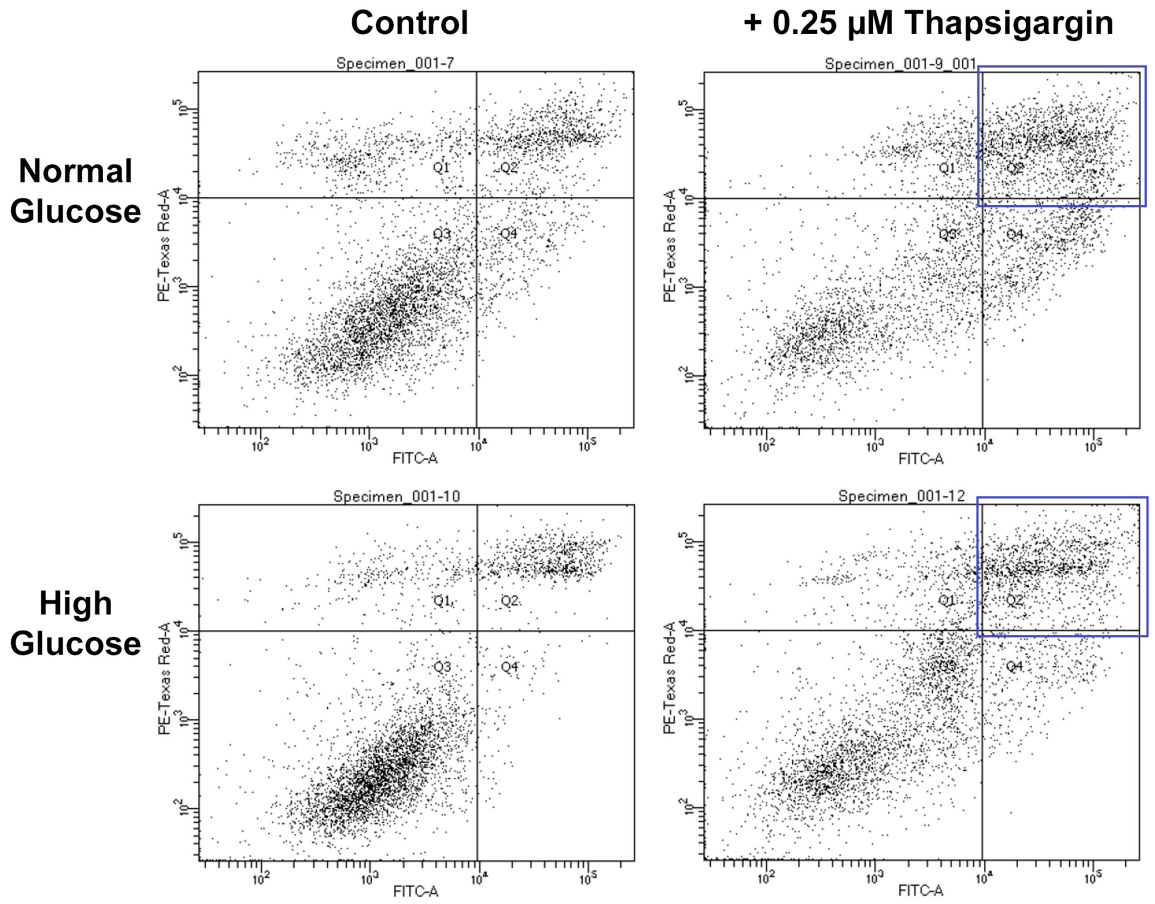

Figure 6. Flow cytometry analysis of cellular apoptosis of thapsigargin treated HCT116 cells. HCT116 cells grown in normal glucose or high glucose were treated with 0.25 μM of thapsigagin for two days and then analyzed by flow cytometry after annexin V and popidium iodide staining. The horizontal axis represents the signal from the staining of FITC-coupled annexin V and the vertical axis represents the signal from popidium iodide staining. The upper right quadrant (frame) represents the apoptotic cells with high staining of annexin V and popidium iodide. The upper left quadrant represents the late stage dying cells with high popidium staining.

ling hyperglycemia might prevent cancer cell proliferation and development of resistance to anti-cancer therapy in patients with T2D and cancer.

In a series of experiments, we confirmed the increased growth of HCT-116 colon cancer cells in high glucose medium which persisted despite switching to normal glucose medium, as evident by activation of genes implicated in cell cycle and cell proliferation. Microarrray analysis implicated activation of the ER stress pathway with varying responses in high glucose and low-glucose medium. The activation of growth promoting pathways and suppression of apoptosis during ER stress might contribute to the cancer cell growth under high glucose medium. Using thapsigargin to induce ER stress, the response was attenuated in cells exposed to high glucose mainly due to reduced apoptosis with reduced levels of cleaved caspase-3. Taken together, our results suggested that high glucose might program cancer cells to adapt the UPR which promotes cell survival with resistance to anti-cancer drugs despite switching to low-glucose medium. These findings may explain the increased cancer risk in patients with T2D and their poor response to anti-cancer treatment [32].

The rate of protein synthesis is determined by the supply of energy and nutrients. Cancer cells have abnormal growth potential and prefer using glucose as an energy substrate [10]. Other researchers had reported the growth-promoting effect of high glucose in MCF7 breast cancer cells accompanied by increased DNA synthesis and activation of cdk2 and cyclin

Table 4. Summary of the effects of Thapsigargin on HCT116 colorectal cancer cells

	Normal glucose		*High glucose*	
	No thapsigargin	+ Thapsigargin	No thapsigargin	+ Thapsigargin
Cell growth and proliferation				
MTT	↑↑	↓↓	↑↑↑	↓
SRB	↑↑	↓↓	↑↑↑	↓
Cycline E2 expression	↑	↑	↑↑↑	↑
Cyclin E2 protein	↑↑	↑	↑↑↑	↑
ER pathway and genes				
ATF4 expression	↑↑	↑↑↑↑	↑↑	↑↑↑
ATF4 protein	↑	↑	↑	↑↑
BIP expression	↑↑	↑↑	↑	↑↑↑
BIP protein	↑↑	↑↑↑↑	↑	↑↑↑
XBP1-v1 mRNA (unspliced)	↑↑	↑↑↑	↑	↑
XBP1-v2 mRNA (spliced)	↑	↑↑↑	↑	↑↑↑
XBP-1s (protein)	↑	↑↑	↑	↑↑↑
Apoptosis genes and response				
TRIB3 expression	↑↑	↑↑↑↑	↑	↑↑↑
Cleaved caspase 3		↑↑↑		↑
Annexin V stained cells		↑↑↑		↑↑

D1 [13, 14]. In our experiments, we demonstrated increased growth of HCT116 cells with activated gene expression implicated in cell cycle progression and DNA replication (*MCM10*, *CLSPN* and *GINS4*). There was also increased expression of cyclin E2 (*CCNE2*) and cdc2 specific phosphatase *CDC25A*, both of which were essential for cell cycle progression from G1 to S phase for DNA synthesis during cell proliferation [33-35]. High glucose also increased the expression of *STAT4* and *MAT2A*. Although *STAT4* is known to respond to growth factor and cytokine stimulation to promote cell proliferation in lymphocytes, activated expression of *STAT4* has been reported in colorectal cancers but not the adjacent normal colon cells [36]. *MAT2A* encodes a methyltransferase for the synthesis of S-adenosylmethionine (SAMe). Increased expression of *MAT2A* has been associated with cancer cells [37]. Given the role of SAMe as the methyl donor in metabolism including the biosynthetic pathways [38], increased expression of *MAT2A* is a sign for activated cell growth and proliferation.

In support of these *in vitro* results demonstrating the growth promoting effects of high glucose, our group has also reported increased *in vivo* growth of transformed tumor cells in *db/db* mice with high blood glucose [39, 40]. In this diabetes-cancer animal model, the tumor size decreased with blood glucose lowering by exendin-4 treatment, which is a glucagon like peptide 1 (GLP1) mimetic with both blood glucose lowering and anti-inflammatory effects [40].

Protein folding is a key process in the configuration of newly synthesized proteins into biologically active proteins. This energy-dependent process requires the assistance of multiple chaperone proteins including BiP (GRP78) [41]. BiP is an ER protein first discovered by its activation by glucose deprivation in many mammalian cells [42]. In keeping with this notion, in our study, we found low BiP expression in cancer cells under high glucose condition.

Other studies confirmed that BiP is a chaperone protein located in the ER normally checked by binding to key signaling molecules including PERK, IRE1 and ATF6. In situation of ER stress, BiP is released from these molecules to bind to unfolded proteins to maintain proper cell functioning by triggering the UPR [18]. As such, the release of these proteins from BiP including ATF6 leads to activation of CHOP. The latter is a key transcription factor for regulating genes which will determine the cellular fate upon failure of ER response [20, 21]. When this ER response is overwhelmed, many CHOP-regu-

lated genes including *TRIB3* can activate the apoptotic pathway while suppression of CHOP can favor cell growth and proliferation [28].

The expressions of the BiP and CHOP genes are regulated by the ER stress response element (ERSE) [43] with both genes having multiple copies of ERSE in their promoter regions [44, 45]. The amount of BiP inside the cell is tightly regulated with release of BiP during UPR to prevent accumulation of unfolded proteins, which if unsuccessful, may trigger cell death. Here, the UPR is mediated by expanding the ER, halting protein synthesis, and degrading the unfolded proteins. These processes can continue as long as there are enough BiP. Thus, since the ratio of unfolded protein load to BiP regulates the amplitude of the UPR, the level of BiP determines the threshold to trigger the UPR [46]. In our experiments using HCT116 cancer cells, we noted high levels of BiP and CHOP in low glucose condition. However, under high glucose condition, the expression of ER-related genes including CHOP, BiP and TRIB3 were reduced. Other researchers have also reported similar findings in MCF7 breast cancer cells [47]. The role of BiP in cancer cells is multi-dimensional. In addition to its role as chaperone protein and ER stress sensor in the ER, BiP can function in the cytosol or present in the cell membrane [48]. BiP can reduce the apoptotic response induced by topoisomerase inhibitors by binding to procaspase-7 [49]. BiP binding partner also includes SPARC (secreted protein, acidic and rich in cysteine). In colon cancer cells, the binding of SPARC to BiP can modulate the interaction between BiP and PERK and IRE1α, resulting in a different UPR signaling that promotes ER stress-associated apoptosis [50]. BiP over expression can confer drug resistance to anti-cancer drugs [51, 52]. In a leukemia cell line developed to resist multiple anti-cancer drugs including thapsigargin, the thapsigargin-resistant cell line also developed resistance to tunicamycin and MG-132, where tunicamycin is an ER stress inducer by blocking protein glycosylation and MG-132 is a proteasome inhibitor [53]. High level of BiP in cancer is not always associated with bad outcome. In a study to evaluate the association of BiP staining in breast cancer and response to chemotherapy, patients with positive BiP staining treated with Adriamycin and Taxane showed lower risk of recurrence [54] but the risk is higher for the BiP positive cancers when the patients were treated with Adriamycin alone [55]. In colon cancer cases evaluated by BiP and SPARC staining, tumors with lower BiP to SPARC ratio showed better outcome with better survival [50]. Taken together, BiP plays a pivotal role in cancer and determines its response to anti-cancer drugs. Our findings suggested that high glucose lowered the level of BiP and thus lowered the threshold for the initiation of the UPR which tended to promote survival of cancer cells.

Thapsigargin is an anti-cancer prodrug which blocks calcium entry into the ER to induce ER stress and UPR culminating into cell death. To explore the cellular fate upon activation of UPR in high glucose condition, we treated cancer cells in normal glucose and cells exposed to high glucose condition with Thapsigargin. In both normal and high glucose conditions, thapsigargin induced increased expression of *ATF4*, splicing of the XBP1 mRNA and CHOP with higher expression of BiP in high glucose condition in HCT116, as a possible mechanism to stabilize the unfolded proteins. Treatment with thapsigargin increased the spliced form of XBP-1 mRNA in both low and high glucose condition. In high glucose condition, the spliced XBP-1 was the main form and the expression of the unspliced form was much lower. A high ratio of spliced to unspliced XBP-1 can perturb multiple metabolic and inflammatory pathways although their roles in promoting cancer growth remains to be defined [22].

Importantly, in high glucose condition, thapsigargin-treated HCT116 showed lower expression of the CHOP regulated gene *TRIB3* than that in low glucose condition. CHOP is the master regulator which maintains a balance between the UPR for cellular protection from unfolded protein and apoptosis pathway when the ER stress is too severe to recover. Cleavage of the caspase-3 is a hallmark and irreversible step in the activation of the apoptosis response [29, 30]. In high glucose condition, we observed reduced level of cleaved caspase-3 in thapsigargin-treated HCT116 cells exposed to high glucose compared with cells treated in normal glucose condition. These divergent responses suggested that high glucose condition facilitated the survival of HCT116 cells despite being challenged with thapsigargin-induced ER stress possibly throu-

gh reduced apoptosis although further studies are required to elucidate the underlying mechanisms. In an animal model of chemically-induced liver cancer in diabetic mice, there was no difference in tumor number although the tumor size was twofold larger with reduced apoptosis compared with tumor in non-diabetic control mice [56]. Taken together, in high glucose condition, cancer cells exhibit lower threshold to trigger UPR which promoted cell growth and survival with reduced apoptosis including resistance to anti-cancer drugs which utilized the ER pathway to induce cell death.

In highly differentiated cell types such as β-cells [16, 17] and cytokine-producing cells [15], high glucose triggered ER stress which can lead to cell death through increased expression of CHOP. Less differentiated cancer cells are programmed to use glucose as the preferred energy source [10, 12]. Our results suggested that high glucose might promote cell proliferation through altered UPR. To this end, glucose deprivation has been shown to reduce cancer cell growth with increased apoptosis [57].

In the 7-year United Kingdom Prospective Diabetes Study which examined the effects of improved glycemic control on risk of complications, patients with poor glycemic control had higher risk of complications which persisted in the 20-year post-trial period despite improvement in glycemic control. This phenomenon was referred as legacy effect or metabolic memory [58, 59]. Apart from having higher risk of cancer, patients with diabetes and cancer have worse clinical outcomes and responses to anti-cancer treatment than those without diabetes [32]. In this context, our results suggested that cancer cells exhibit similar legacy effects with continuing cell growth after exposure to high glucose. Once exposed to high glucose, these cancer cells showed resistance to ER stress induced by thapsigargin despite return to normal glucose condition. In a similar vein, in aortic endothelial cells, transient exposure to high glucose induced chromatin changes in the promoter of the NFκB p65 subunit, resulting in prolonged gene activation which persisted despite return to a normal glucose medium [60]. Several anti-cancer drugs under development, such as Mipsagargin based on thapsigargin, targeted on the dependency of cancer cells on glucose metabolism and altered response to ER stress [61, 62]. Our data suggested that hyperglycemia may attenuate the anti-cancer effects to these treatments.

In conclusion, cancer cells when exposed to high glucose exhibit increased tolerance to ER stress with altered UPR resulting in continuing protein production, increasing cellular proliferation and reduced cellular apoptosis which persisted despite return to normal glucose condition. These programmed cancer cells also showed resistance to anti-cancer drugs which utilize ER pathway to induce cellular apoptosis. These findings may underlie the high risk of cancer in diabetes and their poor response to anti-cancer treatment and emphasize the importance of optimal glycemic control for preventing cancer and improving treatment response to anti-cancer therapies in people with diabetes.

Acknowledgements

We thank Professor Anthony Lo for providing the HCT116 cells and Professor Natalie Wong for her expert advice. We also thank Mr. Wilson Leung, Dr. Stanley Cheung and Mr. Roy Chan for helping out the project. This study was partially supported by an educational grant by Sanofi and the Theme-based Research Scheme (T12-402/13N) and Impact Research Fund by the University Grants Committee of Hong Kong and an educational grant from Sanofi.

Disclosure of conflict of interest

JCNC reported receiving research grants and/or honoraria for consultancy or giving lectures from AstraZeneca, Boehringer Ingelheim, Eli Lilly, Merck Serono, Merck Sharp & Dohme, Pfizer, and Sanofi. RCWM reported receiving grants and/or honoraria for consultancy or giving lectures from AstraZeneca, Bayer, Boehringer Ingelheim, Eli Lilly, Pfizer, and Takeda. APSK has received research grants and/or speaker honoraria from Abbott, AstraZeneca, Eli Lilly, Merck Serono, Nestle, and Novo Nordisk.

Address correspondence to: Juliana Chung Ngor Chan, Department of Medicine and Therapeutics, The Chinese University of Hong Kong, 9/F. Lui Che Woo Clinical Sciences Building, Prince of Wales Hospital, Shatin, N. T. Hong Kong. Tel: +852-35053138; E-mail: jchan@cuhk.edu.hk

References

[1] Greenwood M and Wood F. The relation between the cancer and diabetes death-rates. J Hyg (Lond) 1914; 14: 83-118.

[2] Inoue M, Iwasaki M, Otani T, Sasazuki S, Noda M and Tsugane S. Diabetes mellitus and the risk of cancer: results from a large-scale population-based cohort study in Japan. Arch Intern Med 2006; 166: 1871-1877.

[3] Rao Kondapally Seshasai S, Kaptoge S, Thompson A, Di Angelantonio E, Gao P, Sarwar N, Whincup PH, Mukamal KJ, Gillum RF, Holme I, Njølstad I, Fletcher A, Nilsson P, Lewington S, Collins R, Gudnason V, Thompson SG, Sattar N, Selvin E, Hu FB and Danesh J; Emerging Risk Factors Collaboration. Diabetes mellitus, fasting glucose, and risk of cause-specific death. N Engl J Med 2011; 364: 829-841.

[4] Chan JC, Malik V, Jia W, Kadowaki T, Yajnik CS, Yoon KH and Hu FB. Diabetes in Asia: epidemiology, risk factors, and pathophysiology. JAMA 2009; 301: 2129-2140.

[5] Chan JCN, Lim LL, Luk AOY, Ozaki R, Kong APS, Ma RCW, So WY and Lo SV. From Hong Kong diabetes register to JADE program to RAMP-DM for data-driven actions. Diabetes Care 2019; 42: 2022-2031.

[6] Yang X, So WY, Ma RC, Kong AP, Xu G and Chan JC. Diabetes and cancer: the mechanistic implications of epidemiological analyses from the Hong Kong diabetes registry. Diabetes Metab Res Rev 2012; 28: 379-387.

[7] Yang X, So W, Ko GT, Ma RC, Kong AP, Chow CC, Tong PC and Chan JC. Independent associations between low-density lipoprotein cholesterol and cancer among patients with type 2 diabetes mellitus. CMAJ 2008; 179: 427-437.

[8] Yang X, Ko GT, So WY, Ma RC, Yu LW, Kong AP, Zhao H, Chow CC, Tong PC and Chan JC. Associations of hyperglycemia and insulin usage with the risk of cancer in type 2 diabetes: the Hong Kong diabetes registry. Diabetes 2010; 59: 1254-1260.

[9] Global Burden of Disease Health Financing Collaborator Network. Evolution and patterns of global health financing 1995-2014: development assistance for health, and government, prepaid private, and out-of-pocket health spending in 184 countries. Lancet 2017; 389: 1981-2004.

[10] Warburg O. On respiratory impairment in cancer cells. Science 1956; 124: 269-270.

[11] Kim SY. Cancer energy metabolism: shutting power off cancer factory. Biomol Ther (Seoul) 2018; 26: 39-44.

[12] Dell' Antone P. Energy metabolism in cancer cells: how to explain the Warburg and Crabtree effects? Med Hypotheses 2012; 79: 388-392.

[13] Yamamoto M, Patel NA, Taggart J, Sridhar R and Cooper DR. A shift from normal to high glucose levels stimulates cell proliferation in drug sensitive MCF-7 human breast cancer cells but not in multidrug resistant MCF-7/ADR cells which overproduce PKC-betaII. Int J Cancer 1999; 83: 98-106.

[14] Okumura M, Yamamoto M, Sakuma H, Kojima T, Maruyama T, Jamali M, Cooper DR and Yasuda K. Leptin and high glucose stimulate cell proliferation in MCF-7 human breast cancer cells: reciprocal involvement of PKC-alpha and PPAR expression. Biochim Biophys Acta 2002; 1592: 107-116.

[15] Zhong Y, Li J, Chen Y, Wang JJ, Ratan R and Zhang SX. Activation of endoplasmic reticulum stress by hyperglycemia is essential for Muller cell-derived inflammatory cytokine production in diabetes. Diabetes 2012; 61: 492-504.

[16] Kooptiwut S, Mahawong P, Hanchang W, Semprasert N, Kaewin S, Limjindaporn T and Yenchitsomanus PT. Estrogen reduces endoplasmic reticulum stress to protect against glucotoxicity induced-pancreatic beta-cell death. J Steroid Biochem Mol Biol 2014; 139: 25-32.

[17] Hanchang W, Semprasert N, Limjindaporn T, Yenchitsomanus PT and Kooptiwut S. Testosterone protects against glucotoxicity-induced apoptosis of pancreatic beta-cells (INS-1) and male mouse pancreatic islets. Endocrinology 2013; 154: 4058-4067.

[18] Luo B and Lee AS. The critical roles of endoplasmic reticulum chaperones and unfolded protein response in tumorigenesis and anticancer therapies. Oncogene 2013; 32: 805-818.

[19] Takayanagi S, Fukuda R, Takeuchi Y, Tsukada S and Yoshida K. Gene regulatory network of unfolded protein response genes in endoplasmic reticulum stress. Cell Stress Chaperones 2013; 18: 11-23.

[20] Tabas I and Ron D. Integrating the mechanisms of apoptosis induced by endoplasmic reticulum stress. Nat Cell Biol 2011; 13: 184-190.

[21] Li Y, Guo Y, Tang J, Jiang J and Chen Z. New insights into the roles of CHOP-induced apoptosis in ER stress. Acta Biochim Biophys Sin (Shanghai) 2014; 46: 629-640.

[22] Yadav RK, Chae SW, Kim HR and Chae HJ. Endoplasmic reticulum stress and cancer. J Cancer Prev 2014; 19: 75-88.

[23] Cnop M, Foufelle F and Velloso LA. Endoplasmic reticulum stress, obesity and diabetes. Trends Mol Med 2012; 18: 59-68.

[24] Brattain MG, Fine WD, Khaled FM, Thompson J and Brattain DE. Heterogeneity of malignant cells from a human colonic carcinoma. Cancer Res 1981; 41: 1751-1756.

[25] Vichai V and Kirtikara K. Sulforhodamine B colorimetric assay for cytotoxicity screening. Nat Protoc 2006; 1: 1112-1116.

[26] Mosmann T. Rapid colorimetric assay for cellular growth and survival: application to proliferation and cytotoxicity assays. J Immunol Methods 1983; 65: 55-63.
[27] Lytton J, Westlin M and Hanley MR. Thapsigargin inhibits the sarcoplasmic or endoplasmic reticulum Ca-ATPase family of calcium pumps. J Biol Chem 1991; 266: 17067-17071.
[28] Ohoka N, Yoshii S, Hattori T, Onozaki K and Hayashi H. TRB3, a novel ER stress-inducible gene, is induced via ATF4-CHOP pathway and is involved in cell death. EMBO J 2005; 24: 1243-1255.
[29] Shalini S, Dorstyn L, Dawar S and Kumar S. Old, new and emerging functions of caspases. Cell Death Differ 2015; 22: 526-539.
[30] Savitskaya MA and Onishchenko GE. Mechanisms of apoptosis. Biochemistry (Mosc) 2015; 80: 1393-1405.
[31] Koopman G, Reutelingsperger CP, Kuijten GA, Keehnen RM, Pals ST and van Oers MH. Annexin V for flow cytometric detection of phosphatidylserine expression on B cells undergoing apoptosis. Blood 1994; 84: 1415-1420.
[32] Giovannucci E, Harlan DM, Archer MC, Bergenstal RM, Gapstur SM, Habel LA, Pollak M, Regensteiner JG and Yee D. Diabetes and cancer: a consensus report. Diabetes Care 2010; 33: 1674-1685.
[33] Ray D and Kiyokawa H. CDC25A levels determine the balance of proliferation and checkpoint response. Cell Cycle 2007; 6: 3039-3042.
[34] Payton M, Scully S, Chung G and Coats S. Deregulation of cyclin E2 expression and associated kinase activity in primary breast tumors. Oncogene 2002; 21: 8529-8534.
[35] Jinno S, Suto K, Nagata A, Igarashi M, Kanaoka Y, Nojima H and Okayama H. Cdc25A is a novel phosphatase functioning early in the cell cycle. EMBO J 1994; 13: 1549-1556.
[36] Cheng JM, Yao MR, Zhu Q, Wu XY, Zhou J, Tan WL and Zhan SH. Silencing of stat4 gene inhibits cell proliferation and invasion of colorectal cancer cells. J Biol Regul Homeost Agents 2015; 29: 85-92.
[37] Lu SC and Mato JM. S-adenosylmethionine in cell growth, apoptosis and liver cancer. J Gastroenterol Hepatol 2008; 23 Suppl 1: S73-77.
[38] Schubert HL, Blumenthal RM and Cheng X. Many paths to methyltransfer: a chronicle of convergence. Trends Biochem Sci 2003; 28: 329-335.
[39] He L, Law PT, Boon SS, Zhang C, Ho WC, Banks L, Wong CK, Chan JC and Chan PK. Increased growth of a newly established mouse epithelial cell line transformed with HPV-16 E7 in diabetic mice. PLoS One 2016; 11: e0164490.
[40] He L, Law PTY, Wong CK, Chan JCN and Chan PKS. Exendin-4 exhibits enhanced anti-tumor effects in diabetic mice. Sci Rep 2017; 7: 1791.
[41] Gething MJ. Role and regulation of the ER chaperone BiP. Semin Cell Dev Biol 1999; 10: 465-472.
[42] Shiu RP, Pouyssegur J and Pastan I. Glucose depletion accounts for the induction of two transformation-sensitive membrane proteinsin Rous sarcoma virus-transformed chick embryo fibroblasts. Proc Natl Acad Sci U S A 1977; 74: 3840-3844.
[43] Roy B and Lee AS. The mammalian endoplasmic reticulum stress response element consists of an evolutionarily conserved tripartite structure and interacts with a novel stress-inducible complex. Nucleic Acids Res 1999; 27: 1437-1443.
[44] Yoshida H, Okada T, Haze K, Yanagi H, Yura T, Negishi M and Mori K. ATF6 activated by proteolysis binds in the presence of NF-Y (CBF) directly to the cis-acting element responsible for the mammalian unfolded protein response. Mol Cell Biol 2000; 20: 6755-6767.
[45] Yoshida H, Haze K, Yanagi H, Yura T and Mori K. Identification of the cis-acting endoplasmic reticulum stress response element responsible for transcriptional induction of mammalian glucose-regulated proteins. Involvement of basic leucine zipper transcription factors. J Biol Chem 1998; 273: 33741-33749.
[46] Bakunts A, Orsi A, Vitale M, Cattaneo A, Lari F, Tade L, Sitia R, Raimondi A, Bachi A and van Anken E. Ratiometric sensing of BiP-client versus BiP levels by the unfolded protein response determines its signaling amplitude. Elife 2017; 6: e27518.
[47] Kretowski R, Borzym-Kluczyk M, Stypulkowska A, Branska-Januszewska J, Ostrowska H and Cechowska-Pasko M. Low glucose dependent decrease of apoptosis and induction of autophagy in breast cancer MCF-7 cells. Mol Cell Biochem 2016; 417: 35-47.
[48] Misra UK, Deedwania R and Pizzo SV. Activation and cross-talk between Akt, NF-kappaB, and unfolded protein response signaling in 1-LN prostate cancer cells consequent to ligation of cell surface-associated GRP78. J Biol Chem 2006; 281: 13694-13707.
[49] Reddy RK, Mao C, Baumeister P, Austin RC, Kaufman RJ and Lee AS. Endoplasmic reticulum chaperone protein GRP78 protects cells from apoptosis induced by topoisomerase inhibitors: role of ATP binding site in suppression of caspase-7 activation. J Biol Chem 2003; 278: 20915-20924.
[50] Chern YJ, Wong JCT, Cheng GSW, Yu A, Yin Y, Schaeffer DF, Kennecke HF, Morin G and Tai IT.

The interaction between SPARC and GRP78 interferes with ER stress signaling and potentiates apoptosis via PERK/eIF2alpha and IRE-1alpha/XBP-1 in colorectal cancer. Cell Death Dis 2019; 10: 504.

[51] Pyrko P, Schonthal AH, Hofman FM, Chen TC and Lee AS. The unfolded protein response regulator GRP78/BiP as a novel target for increasing chemosensitivity in malignant gliomas. Cancer Res 2007; 67: 9809-9816.

[52] Virrey JJ, Dong D, Stiles C, Patterson JB, Pen L, Ni M, Schonthal AH, Chen TC, Hofman FM and Lee AS. Stress chaperone GRP78/BiP confers chemoresistance to tumor-associated endothelial cells. Mol Cancer Res 2008; 6: 1268-1275.

[53] Cagala M, Pavlikova L, Seres M, Kadlecikova K, Breier A and Sulova Z. Development of resistance to endoplasmic reticulum stress-inducing agents in mouse leukemic L1210 cells. Molecules 2020; 25: 2517.

[54] Lee E, Nichols P, Groshen S, Spicer D and Lee AS. GRP78 as potential predictor for breast cancer response to adjuvant taxane therapy. Int J Cancer 2011; 128: 726-731.

[55] Lee E, Nichols P, Spicer D, Groshen S, Yu MC and Lee AS. GRP78 as a novel predictor of responsiveness to chemotherapy in breast cancer. Cancer Res 2006; 66: 7849-7853.

[56] Yamasaki K, Hayashi Y, Okamoto S, Osanai M and Lee GH. Insulin-independent promotion of chemically induced hepatocellular tumor development in genetically diabetic mice. Cancer Sci 2010; 101: 65-72.

[57] Iurlaro R, Puschel F, Leon-Annicchiarico CL, O'Connor H, Martin SJ, Palou-Gramon D, Lucendo E and Munoz-Pinedo C. Glucose deprivation induces ATF4-mediated apoptosis through TRAIL death receptors. Mol Cell Biol 2017; 37: e00479-16.

[58] Holman RR, Paul SK, Bethel MA, Matthews DR and Neil HA. 10-year follow-up of intensive glucose control in type 2 diabetes. N Engl J Med 2008; 359: 1577-1589.

[59] Control Group, Turnbull FM, Abraira C, Anderson RJ, Byington RP, Chalmers JP, Duckworth WC, Evans GW, Gerstein HC, Holman RR, Moritz TE, Neal BC, Ninomiya T, Patel AA, Paul SK, Travert F and Woodward M. Intensive glucose control and macrovascular outcomes in type 2 diabetes. Diabetologia 2009; 52: 2288-2298.

[60] El-Osta A, Brasacchio D, Yao D, Pocai A, Jones PL, Roeder RG, Cooper ME and Brownlee M. Transient high glucose causes persistent epigenetic changes and altered gene expression during subsequent normoglycemia. J Exp Med 2008; 205: 2409-2417.

[61] Mahalingam D, Wilding G, Denmeade S, Sarantopoulas J, Cosgrove D, Cetnar J, Azad N, Bruce J, Kurman M, Allgood VE and Carducci M. Mipsagargin, a novel thapsigargin-based PSMA-activated prodrug: results of a first-in-man phase I clinical trial in patients with refractory, advanced or metastatic solid tumours. Br J Cancer 2016; 114: 986-994.

[62] Andersen TB, Lopez CQ, Manczak T, Martinez K and Simonsen HT. Thapsigargin--from thapsia L. to mipsagargin. Molecules 2015; 20: 6113-6127.